eLIFE
elifesciences.org

Figures and figure supplements

Resveratrol modulates the inflammatory response via an estrogen receptor-signal integration network

Jerome C Nwachukwu, et al.

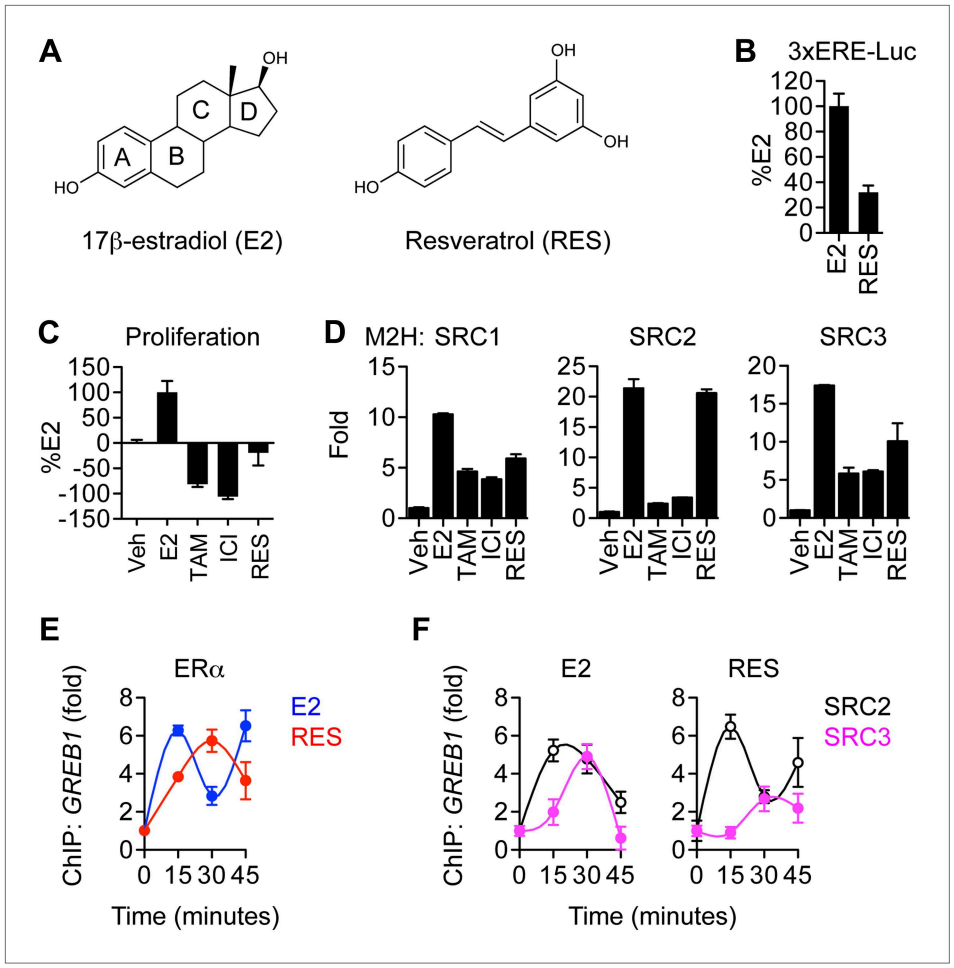

Figure 1. Effects of resveratrol on the canonical ERα proliferative pathway. (**A**) Chemical structures of E2 and resveratrol. (**B**) Luciferase assay of MCF-7 cells transfected with 3xERE-luciferase reporter and stimulated with 10 nM E2 or 10 μM resveratrol. (**C**) Steroid-deprived MCF-7 cells were treated with 10 nM E2, 10 μM 4-hydroxytamoxifen (TAM), 10 μM ICI182, 780, or 10 μM resveratrol. After 7 days, cell number was determined with a standard curve. (**D**) Mammalian two-hybrid assays with ERα and the coactivators SRC1-3. HEK293-T cells were transfected with Gal4 SRC1-3 fusions, ERα-VP-16, and the 5xUAS-luciferase reporter for 24 hr. Cells were treated with 10 nM E2, 10 μM TAM, 10 μM ICI, or 10 μM resveratrol for 24 hr and processed for luciferase activity. Data are presented in panels **B**–**D** as mean ± SEM. (**E**) Resveratrol-induced recruitment of ERα to the *GREB1* promoter. Occupancy of *GREB1* by ERα was compared by ChIP assay in MCF-7 cells that were steroid deprived for 3 days, treated with 10 nM E2 or 10 μM resveratrol, and fixed after 0, 15, 30, or 45 min (mean ± SEM *n* = 2). (**F**) Resveratrol reduced SRC3 but not SRC2 recruitment at the *GREB1* promoter. Occupancy of *GREB1* by SRC2 and SRC3 were examined by ChIP assay in MCF-7 cells treated as described in panel **A**. Average promoter occupancies are shown as fold changes (mean ± SEM *n* = 2).

DOI: 10.7554/eLife.02057.003

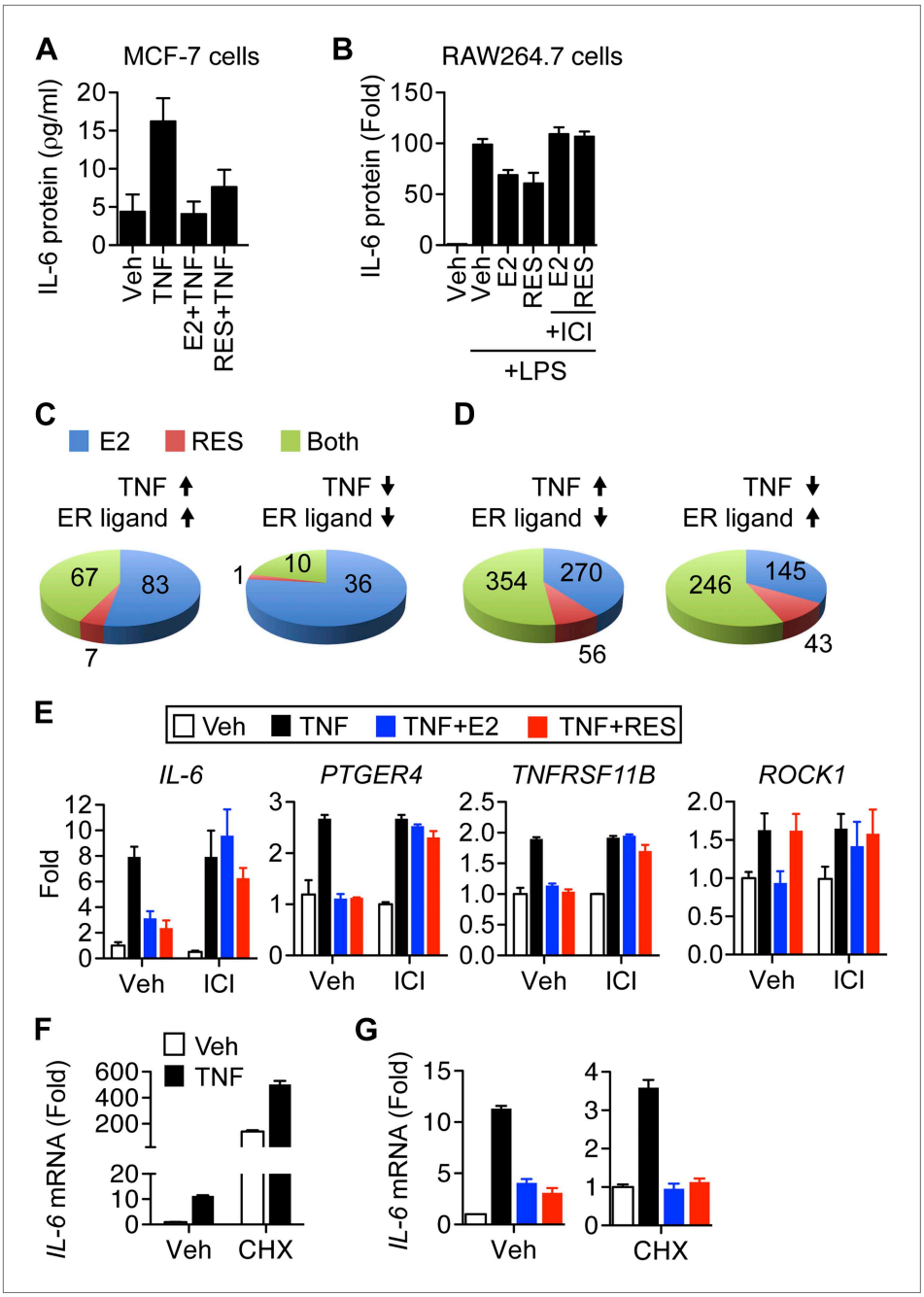

Figure 2. Resveratrol represses inflammatory genes through ER. (**A**) MCF-7 cells were plated into charcoal-stripped phenol red free media and treated for 24 hr with 1 ng/ml TNFα ±10 μM E2, or 10 μM resveratrol. Secreted IL-6 protein was measured from the media using AlphaLISA. Mean ± SEM of biological triplicates are shown. (**B**) RAW264.7 macrophages were treated as in panel **A**, and stimulated with LPS as indicated. Mean ± SEM from biological triplicates are shown. (**C** and **D**) Steroid-deprived MCF-7 cells were treated for 4 hr with 10 ng/ml TNFα alone or in combination with 10 nM E2 or 10 μM resveratrol. Total RNA was reverse transcribed and analyzed using Affymetrix Genechip microarrays. Transcripts showing ≥twofold changes in expression upon TNFα stimulation were classified as indicated. Summary of genes regulated (**C**) in the same direction or (**D**) in opposite directions by TNFα and ER ligands are shown. (**E**) Steroid-deprived MCF-7 were pre-treated for 1 hr with ethanol vehicle or 1 μM ICI, and then treated as indicated with 10 ng/ml TNFα, 10 nM E2, and 10 μM resveratrol for 2 hr. Total RNA reverse-transcribed and analyzed by qPCR for the indicated mRNAs. Mean ± SEM of a representative experiment of biological duplicates are shown. (**F** and **G**) *IL-6* mRNA levels in steroid-deprived MCF-7 cells pre-treated with vehicle or 10 μg/ml CHX for 1 hr and stimulated TNFα, E2, and resveratrol as in panel **D** for 3 hr were analyzed by

Figure 2. Continued on next page

Figure 2. Continued

qPCR. Levels in the control samples (first bar) of each graph were arbitrarily set to 1. Mean ± SEM of a representative experiment are shown.

DOI: 10.7554/eLife.02057.004

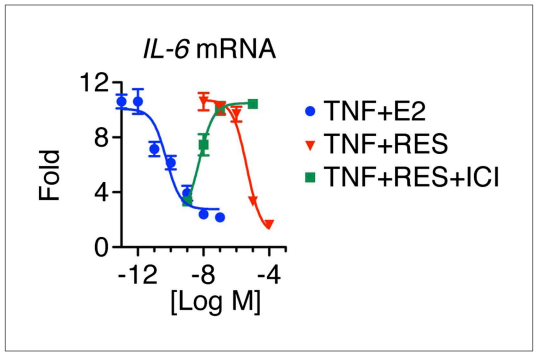

Figure 2—figure supplement 1. Resveratrol represses *IL-6* in a dose-dependent manner.

DOI: 10.7554/eLife.02057.005

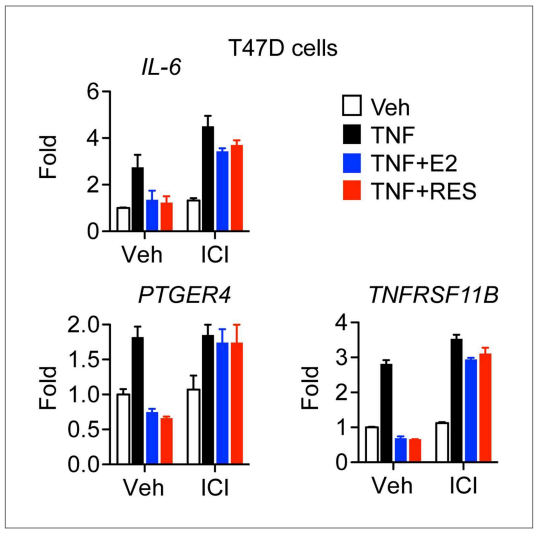

Figure 2—figure supplement 2. Resveratrol represses inflammatory genes through ER.

DOI: 10.7554/eLife.02057.006

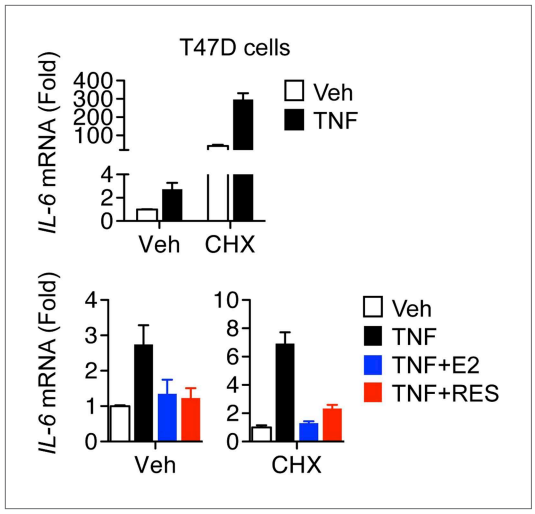

Figure 2—figure supplement 3. Resveratrol represses *IL-6* in cycloheximide-treated cells.
DOI: 10.7554/eLife.02057.007

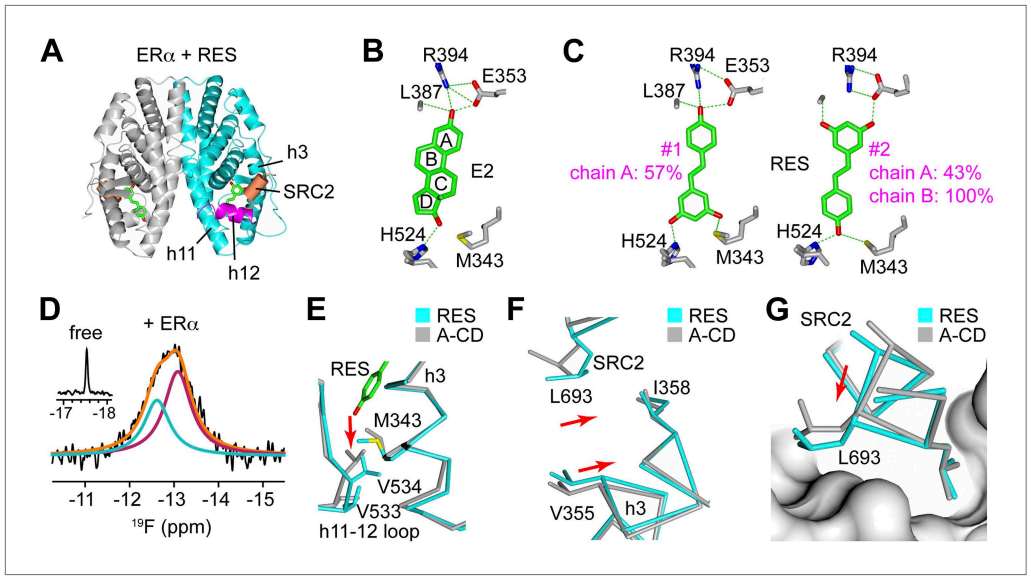

Figure 3. ERα adopts a resveratrol-specific conformation. (**A**) Crystal structure of ERα LBD in complex with resveratrol. The LBD is shown as a ribbon diagram with one monomer colored gray and the other cyan, except for helix 12 (h12), colored magenta. The receptor-interacting peptide of SRC2 (coral tube) docks at the AF2 surface. (**B**) Structure of E2-bound ERα shows that the A-ring forms a hydrogen-bonding network that is conserved among steroid receptors. PDB ID: 1ERE. (**C**) Binding orientations of resveratrol. Compared to E2, resveratrol binds in two distinct orientations. Conformer #1 shows the expected binding orientation, with the phenol mimicking the A-ring of E2. In contrast, the 'flipped' conformer #2 with the resorcinol mimicking the A-ring of E2 was unexpected and predominant. Hydrogen bonds (dashes) and residues that contact the resveratrol molecule are shown. (**D**) ^{19}F-NMR of F-resveratrol. The inset shows a narrow peak in the spectrum of F-resveratrol in buffer (half-height line width = 27 Hz), while the broad peak for F-resveratrol bound to ERα LBD (modeled in orange) fits best to two NMR resonances (colored red and blue), consistent with two distinct binding modes. (**E**–**G**) Crystal structure of the ERα LBD in complex with the control compound i.e., an A-CD ring estrogen (gray), was superposed on the resveratrol-bound structure (cyan). In panel **E**, resveratrol (green) shifts h3 Met343 to disrupt the normal packing of the h11–h12 loop, shifting the position of V534 by 2.5 Å. In panel **F**, resveratrol-induced shift in h3 is transmitted allosterically via ERαV355 and ERα I358 to SRC2 L693 within its ^{690}LxxLL^{694} motif. Panel **G** shows the resveratrol-induced rotation of the SRC2 peptide.
DOI: 10.7554/eLife.02057.008

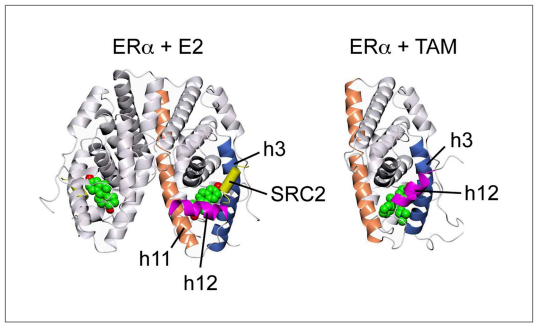

Figure 3—figure supplement 1. Crystal structures of the ERα LBD in complex with E2 and 4-hydroxytamoxifen (TAM).

DOI: 10.7554/eLife.02057.009

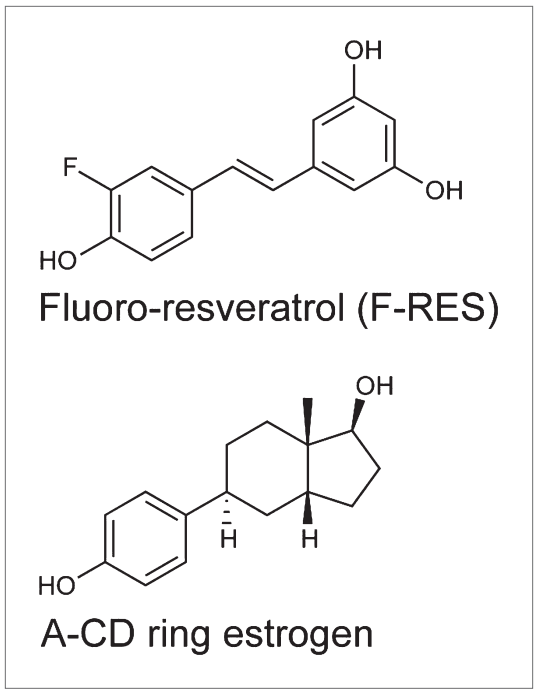

Figure 3—figure supplement 2. Chemical structures of F-resveratrol and the A-CD ring estrogen used as a structural control.

DOI: 10.7554/eLife.02057.010

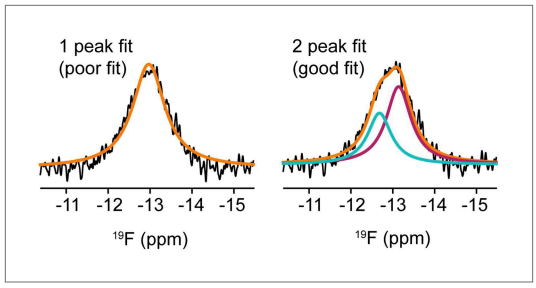

Figure 3—figure supplement 3. Deconvolution of NMR signal from F-resveratrol bound to ERα.
DOI: 10.7554/eLife.02057.011

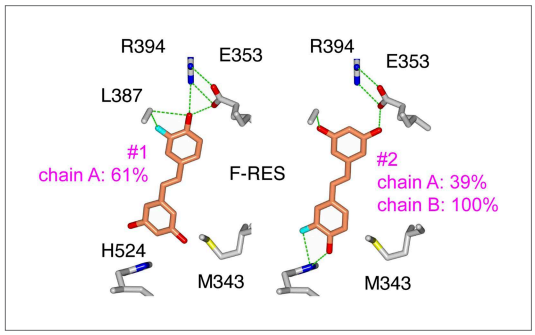

Figure 3—figure supplement 4. F-RES also binds ERα in two orientations.
DOI: 10.7554/eLife.02057.012

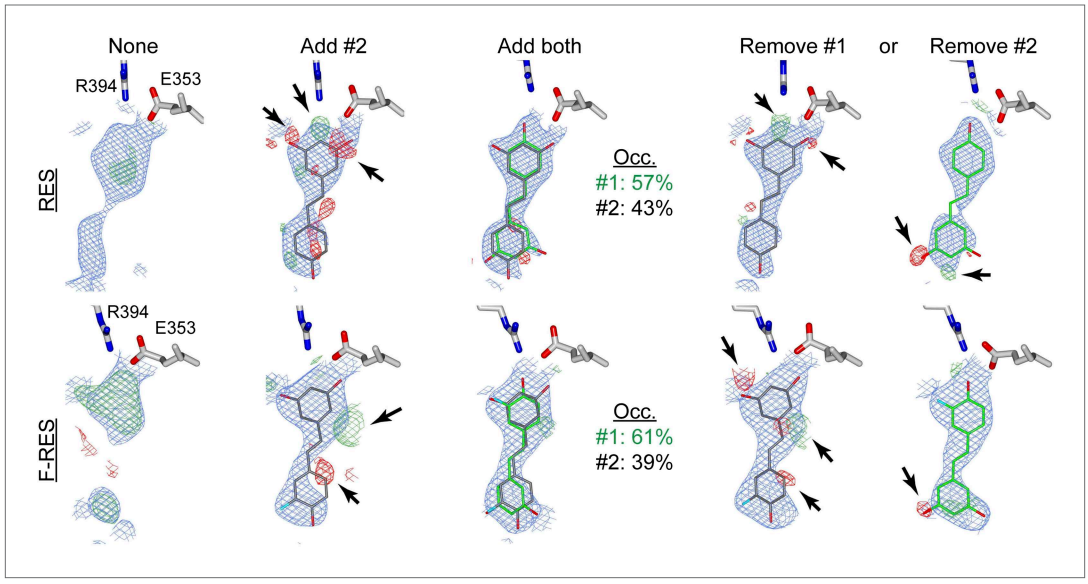

Figure 3—figure supplement 5. Electron density maps of resveratrol and F-resveratrol within the ERα ligand-binding pocket.
DOI: 10.7554/eLife.02057.013

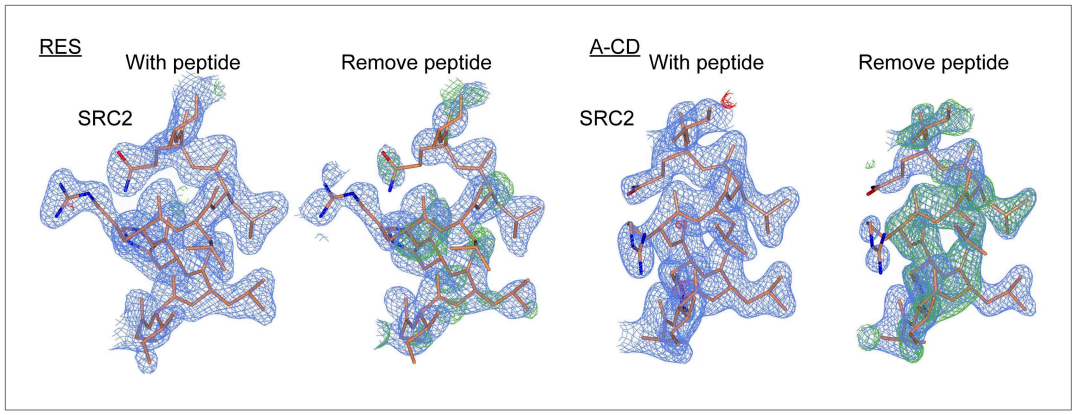

Figure 3—figure supplement 6. Electron density maps of SRC2 peptides docked at the AF2 surface.
DOI: 10.7554/eLife.02057.014

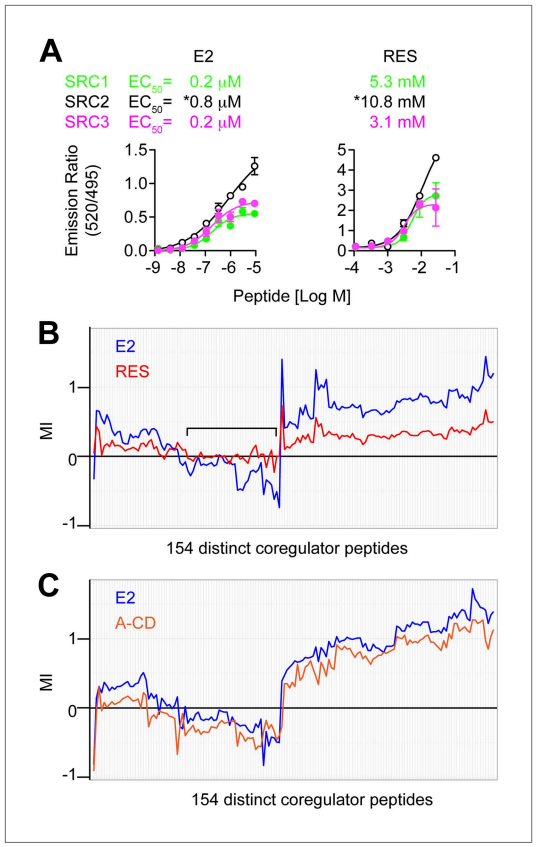

Figure 4. Resveratrol alters the binding of coregulator peptides to the ERα LBD. (**A**) E2- and resveratrol-induced binding of SRC1, SRC2, and SRC3 peptides to the ERα LBD were compared using LanthaScreen assay performed at fixed ligand concentrations, with increasing doses of SRC peptides. Mean ± SEM (n = 3) are shown. *EC_{50} could not be determined accurately since the saturating SRC2 peptide dose is unclear. (**B** and **C**) Hierarchical clustering of coregulator peptide-binding at the AF2 surface induced by 1 μM E2, (**B**) 100 μM resveratrol or (**C**) 1 μM A-CD ring estrogen, was performed using the quantitative in vitro assay, MARCoNI. MI >0 suggests ligand-induced recruitment, while MI <0 suggests ligand-dependent dismissal of a peptide compared to DMSO vehicle. The black bracket shows a cluster of E2 dismissed peptides that are not dismissed by resveratrol. See ***Figure 4—figure supplement 2*** for more details.

DOI: 10.7554/eLife.02057.016

SRC1 peptide ^{683}LTERHKILHRLLQEGSPSD^{701}
SRC2 peptide ^{683}LKEKHKILHRLLQDSSSPV^{701}
SRC3 peptide ^{614}ESKGHKKLLQLLTCSSDDR^{632}

Figure 4—figure supplement 1. SRC peptides.

DOI: 10.7554/eLife.02057.017

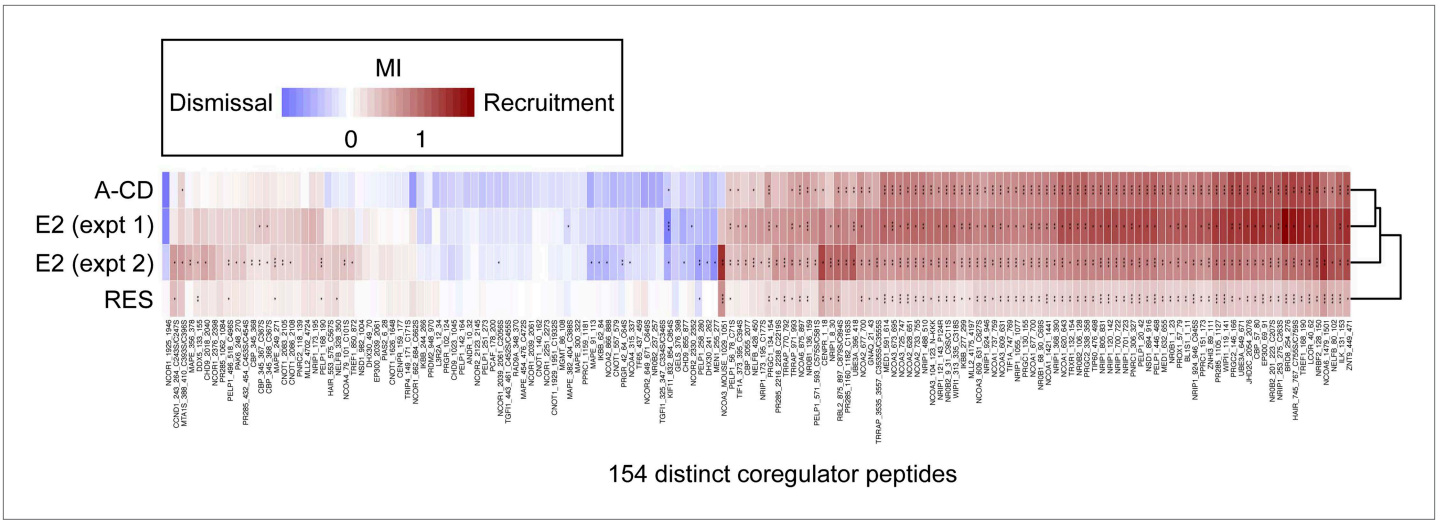

Figure 4—figure supplement 2. Details of proteomic comparison of ligand-induced binding of coregulator peptides using MARCoNI.
DOI: 10.7554/eLife.02057.018

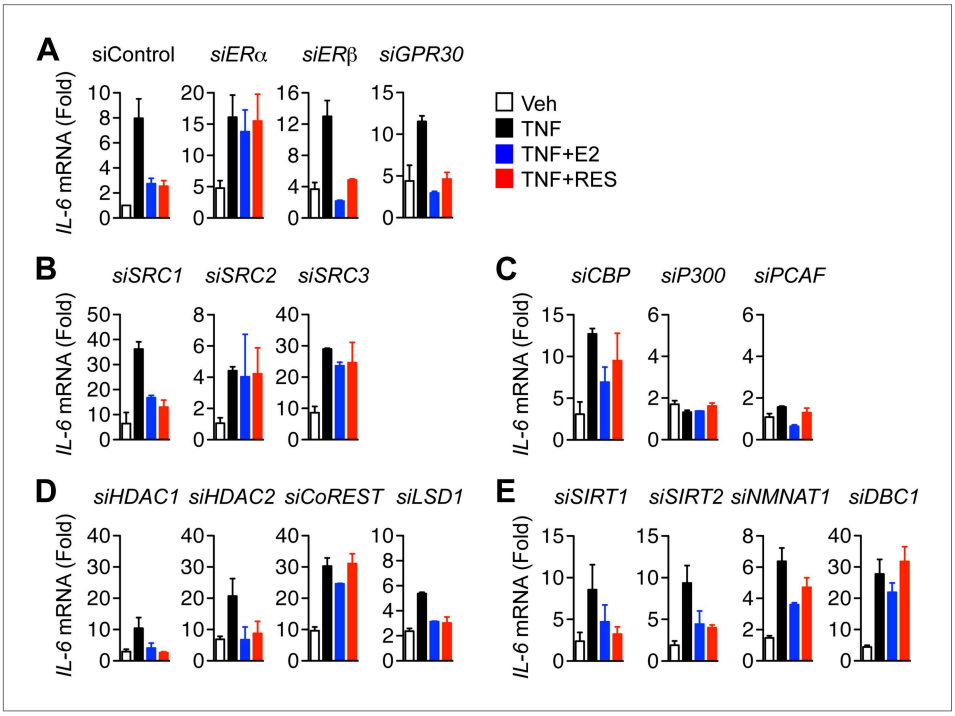

Figure 5. Molecular requirements for resveratrol- and E2-mediated suppression of *IL-6*. (**A**–**E**) MCF-7 cells were transfected with the indicated siRNAs and steroid-deprived for 48 hr. The cells were then treated with 10 ng/ml TNFα and 10 μM resveratrol or 10 nM E2 for 2 hr. *IL-6* mRNA levels were compared by qPCR, and are shown relative to the cells treated with ethanol vehicle and control siRNA. The small-scale siRNA screen was repeated three different times. Mean ± SEM are shown.
DOI: 10.7554/eLife.02057.019

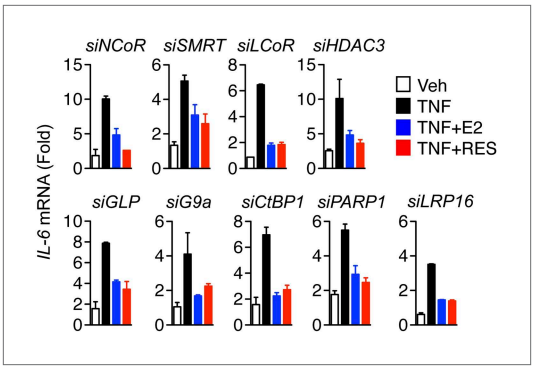

Figure 5—figure supplement 1. Molecular requirements for resveratrol- and E2-mediated suppression of *IL-6*.
DOI: 10.7554/eLife.02057.020

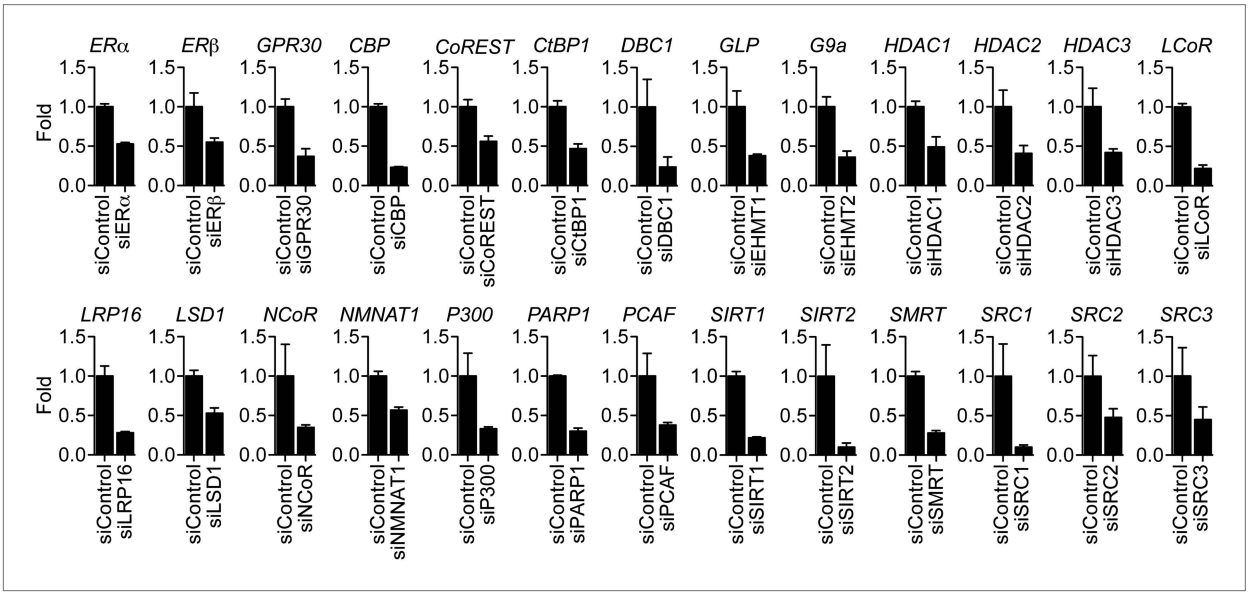

Figure 5—figure supplement 2. Effect of siRNAs on target mRNA levels.
DOI: 10.7554/eLife.02057.021

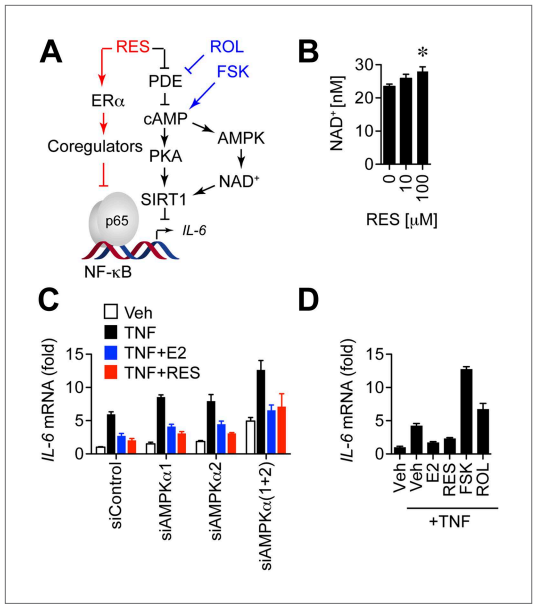

Figure 6. Resveratrol does not repress IL-6 through the cAMP or AMPK pathways. (**A**) Resveratrol stimulates ERα activity and inhibits cAMP-specific phosphodiesterases (PDEs) to activate cAMP SIRT1, and AMPK. The small molecule compounds i.e., the adenylyl cyclase activator forskolin (FSK) and the PDE inhibitor rolipram (ROL) used to further dissect this signaling network are shown in blue. (**B**) Resveratrol increases intracellular NAD^+ levels. Average intracellular NAD^+ concentrations were determined in MCF-7 cells treated with resveratrol for 5 min. Unpaired Student's *t* test (mean ± SEM, *n* = 6) was used to determine statistical significance. *p=0.006. (**C**) *IL-6* mRNA levels in steroid-deprived MCF-7 cells transfected with the indicated siRNAs and treated as described in ***Figure 5***, were compared by qPCR. Mean ± SEM of representative biological duplicates are shown. (**D**) Steroid-deprived MCF-7 cells were treated with 10 ng/ml TNFα, 10 nM E2, 10 μM resveratrol, 10 μM FSK, and 25 μM ROL as indicated for 2 hr. Relative *IL-6* mRNA levels were compared by qPCR. Mean ± SEM of representative biological duplicates are shown.

DOI: 10.7554/eLife.02057.022

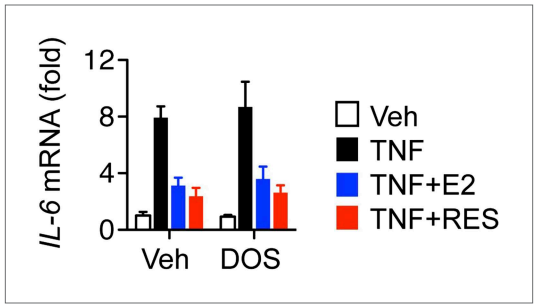

Figure 6—figure supplement 1. Resveratrol represses *IL-6* in cells dorsomorphin-treated cells.

DOI: 10.7554/eLife.02057.023

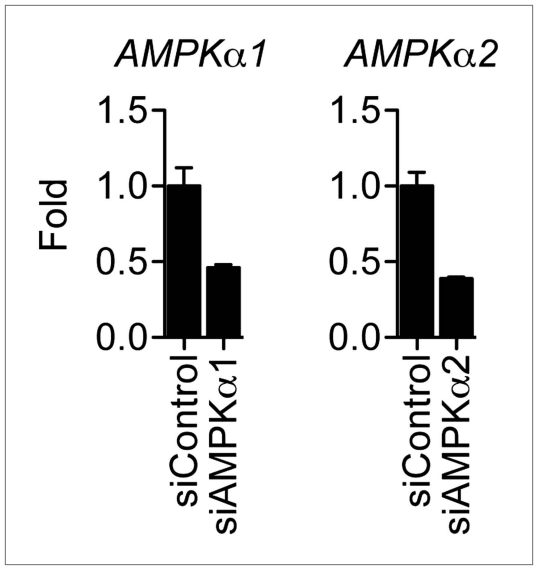

Figure 6—figure supplement 2. Effect of siRNAs on the mRNA levels of AMPK catalytic subunits.
DOI: 10.7554/eLife.02057.024

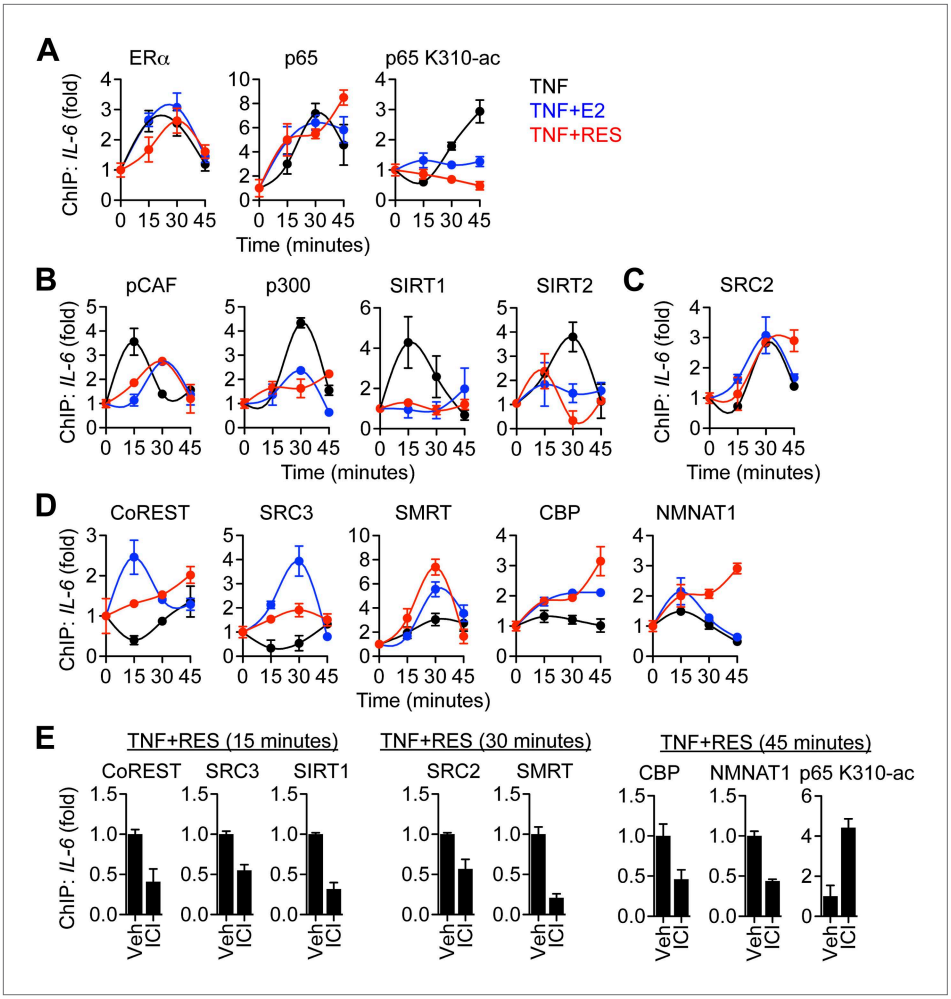

Figure 7. ERα orchestrates ligand-dependent coregulator exchange at the *IL-6* promoter. (**A**–**D**) Occupancy of the indicated factors at the *IL-6* promoter were compared by ChIP assay in steroid-deprived MCF-7 cells treated with 10 ng/ml TNFα alone or in combination with 10 nM E2 or 10 μM resveratrol, and fixed after 0, 15, 30, and 45 min (mean ± SEM *n* = 3) (**E**) Effect of ICI on promoter occupancy was determined by ChIP assay in steroid-deprived MCF-7 cells were pretreated with vehicle or 1 μM ICI for 1 hr, stimulated with 10 ng/ml TNFα plus 10 μM resveratrol, and fixed after 15, 30, or 45 min. Average promoter occupancies are shown as fold changes (mean ± SEM *n* = 3).
DOI: 10.7554/eLife.02057.025

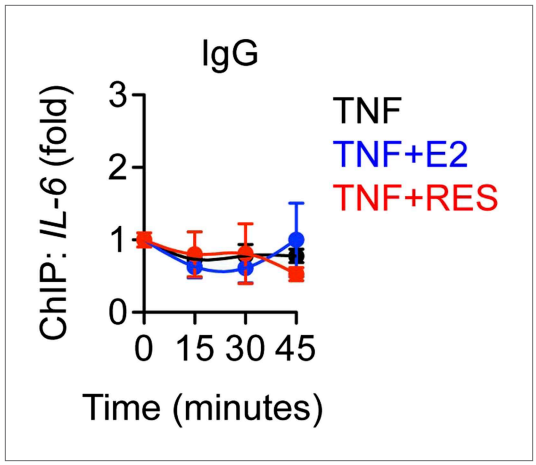

Figure 7—figure supplement 1. Control ChIP assay.
DOI: 10.7554/eLife.02057.026

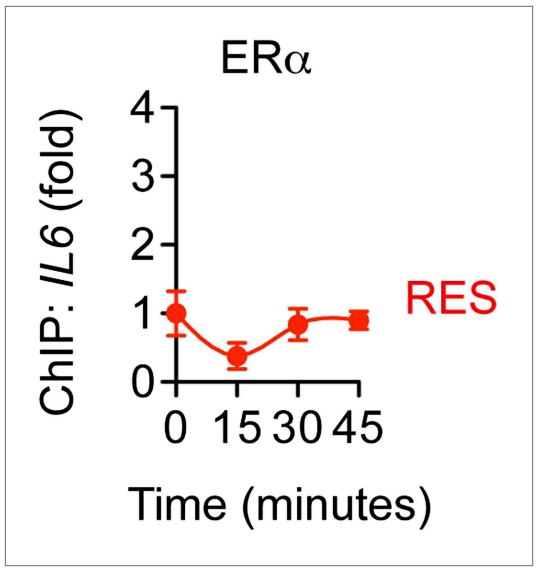

Figure 7—figure supplement 2. Without TNFα, RES does not induce recruitment of ERα to the *IL-6* promoter.
DOI: 10.7554/eLife.02057.027

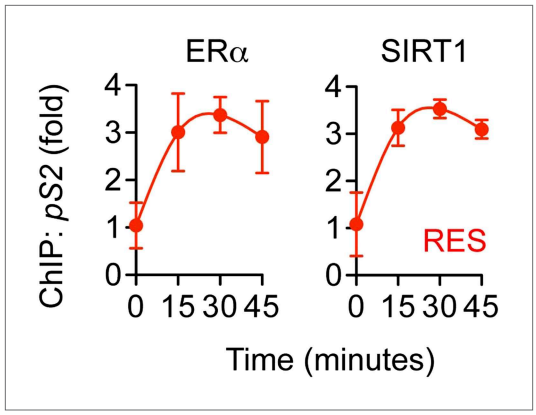

Figure 7—figure supplement 3. RES induces ERα and SIRT1 recruitment at the *TFF1/pS2* promoter.
DOI: 10.7554/eLife.02057.028

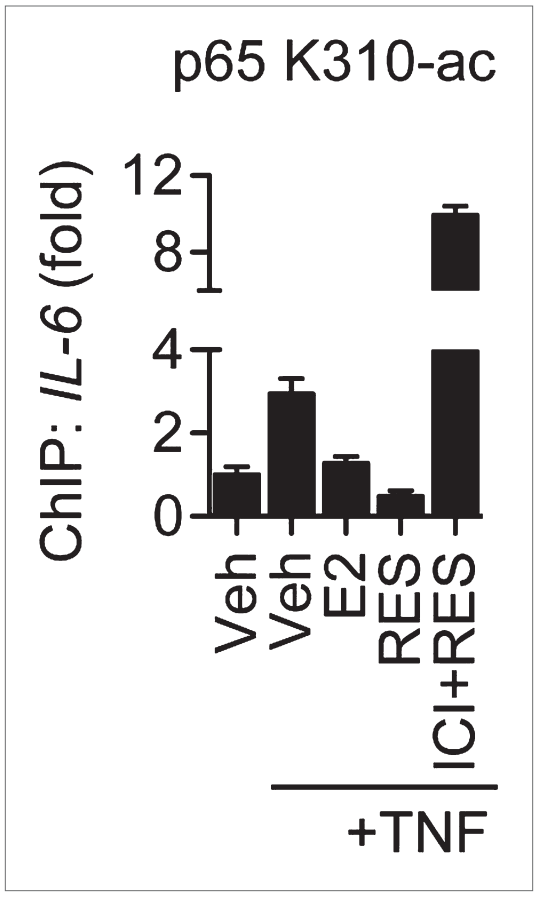

Figure 7—figure supplement 4. ICI increased p65 K310-ac levels at the *IL-6* promoter.
DOI: 10.7554/eLife.02057.029

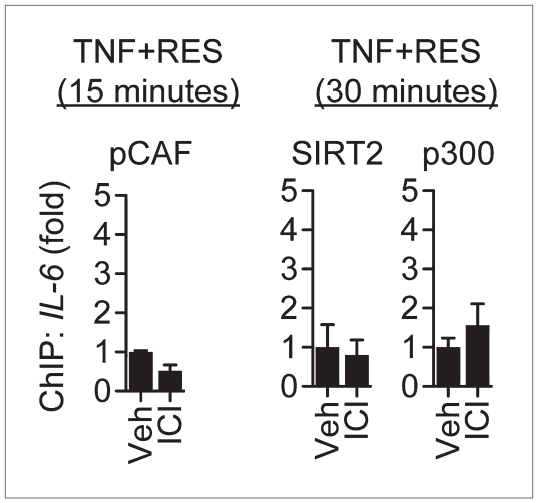

Figure 7—figure supplement 5. ICI did not increase recruitment of pCAF, p300 and SIRT2.
DOI: 10.7554/eLife.02057.030

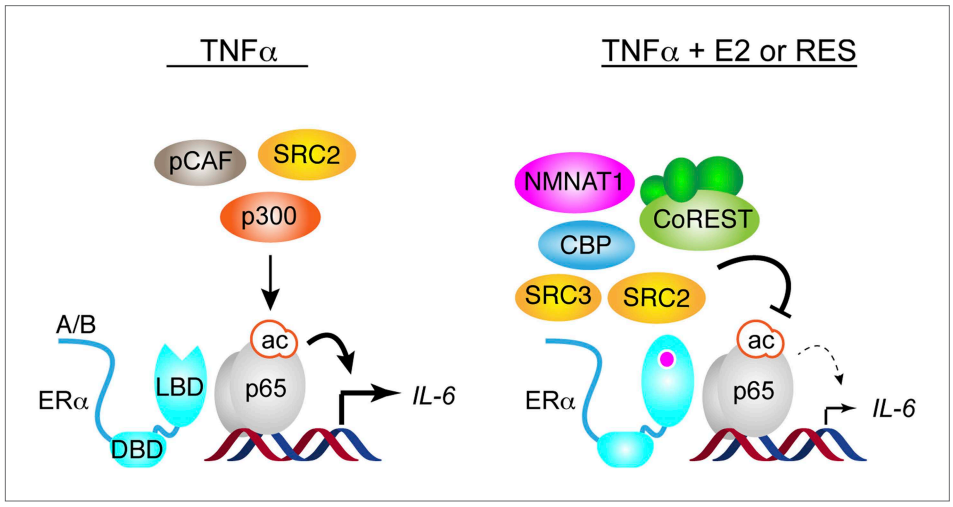

Figure 8. Proposed model for ERα-mediated transrepression of *IL-6*. In MCF-7 cells stimulated with TNFα, the p65 NF-κB subunit binds the *IL-6* promoter and mediates recruitment of many coregulators including p300, which acetylates p65 at Lys310, to drive transactivation of *IL-6*. In these cells, TNFα also induces recruitment of ERα to this site via a tethering mechanism. In response to E2 or resveratrol, ERα undergoes a conformational change, dismisses the set of coregulators including p300, and recruits a set that contains SRC3, CoREST, and other key coregulators required to inhibit p65 acetylation and repress *IL-6*.
DOI: 10.7554/eLife.02057.031

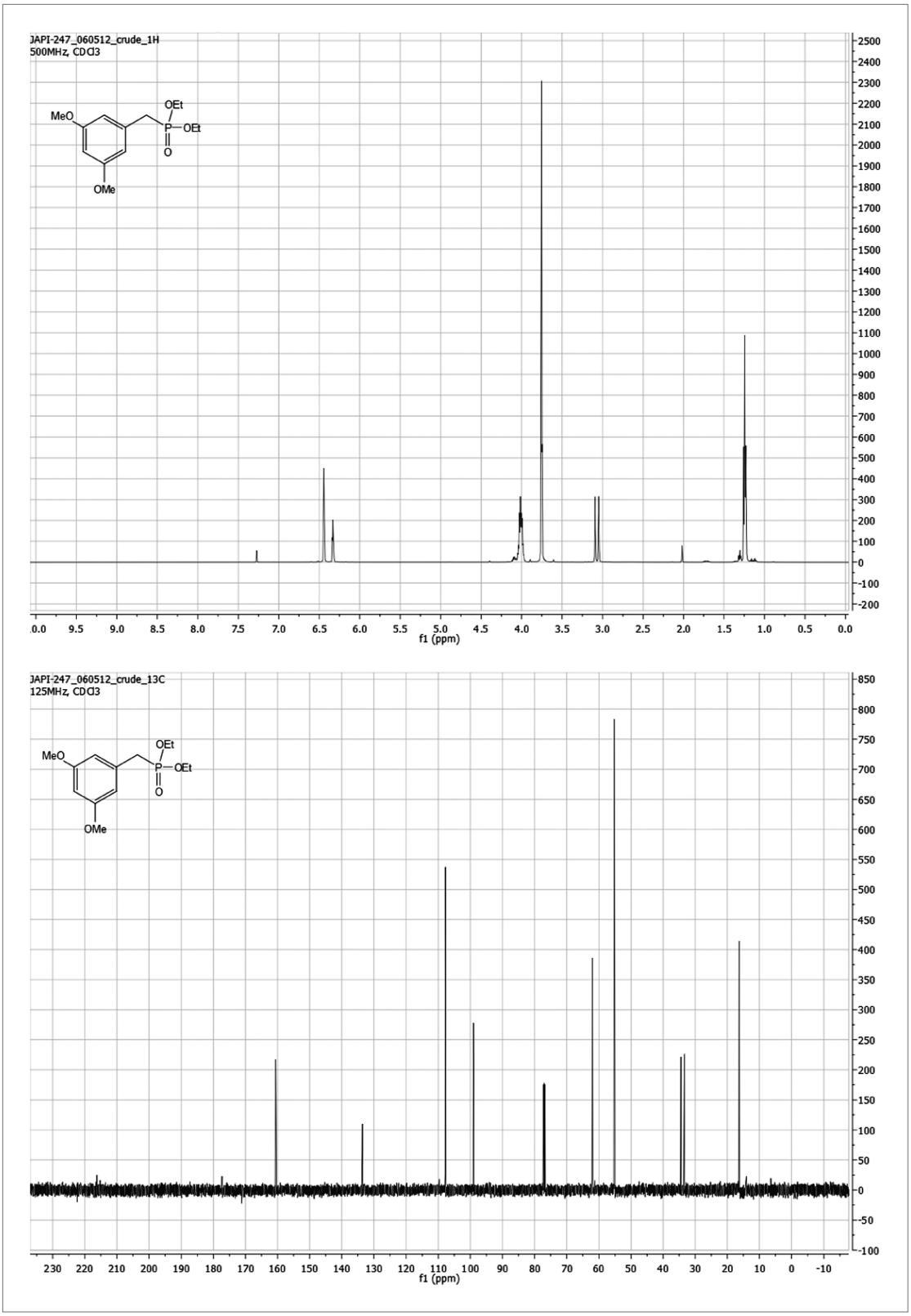

Figure 9. Diethyl 3,5-dimethoxybenzylphosphonate S1.
DOI: 10.7554/eLife.02057.034

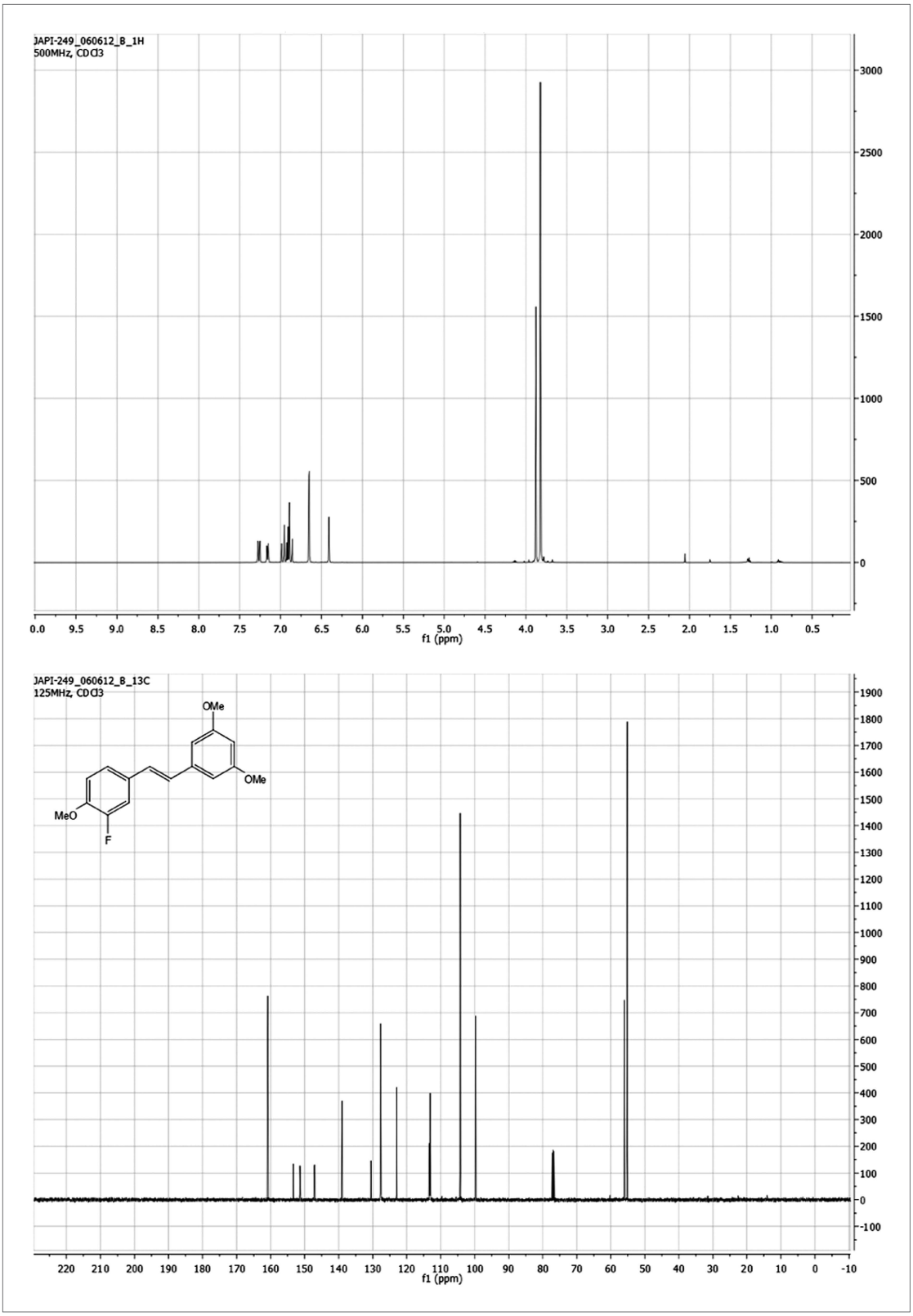

Figure 10. *(E)*-1-(3-fluoro-4-methoxystyryl)-3,5-dimethoxybenzene S2.
DOI: 10.7554/eLife.02057.035

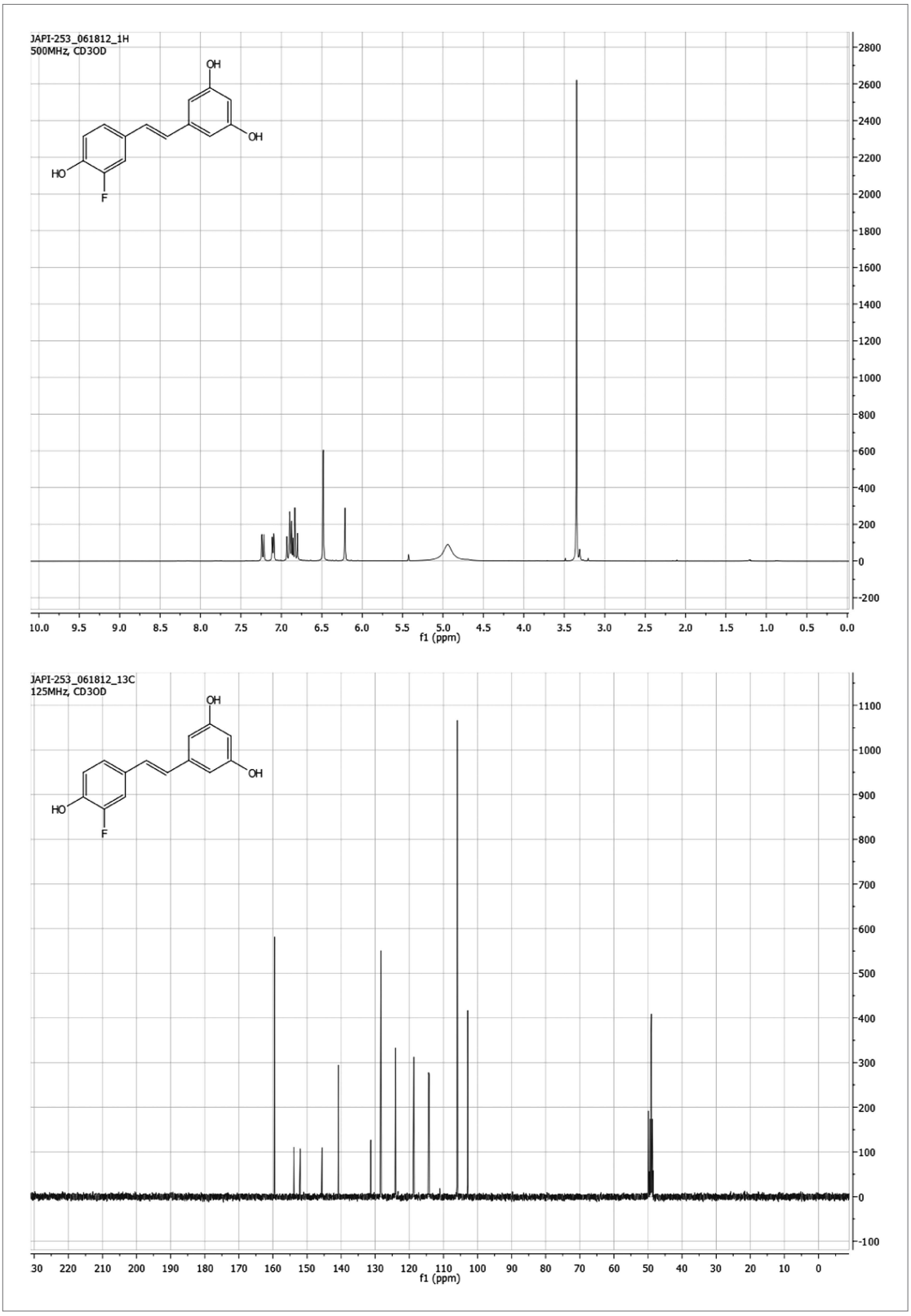

Figure 11. *(E)*-5-(3-fluoro-4-hydroxystyryl)benzene-1,3-diol F-Resveratrol.
DOI: 10.7554/eLife.02057.036